Confidential

Study of a coaxial thermo acoustic-Stirling cooler

M.E.H. Tijani

S. spoelstra

Published in Cryogenics 48 (2008), 77-82

ECN-W--08-013 JUNE 2008

Available online at www.sciencedirect.com
ScienceDirect
Cryogenics 48 (2008) 77–82
CRYOGENICS
www.elsevier.com/locate/cryogenics

Study of a coaxial thermoacoustic-Stirling cooler

M.E.H. Tijani *, S. Spoelstra

Energy research Centre of the Netherlands (ECN), P.O. Box 1, 1755 ZG Petten, The Netherlands

Received 28 August 2007; received in revised form 10 December 2007; accepted 9 January 2008

Abstract

A coaxial thermoacoustic-Stirling cooler is built and performance measurements are performed. The cooler uses the acoustic power produced by a linear motor to pump heat through a regenerator from a cold heat exchanger to an ambient one. The cooler incorporates a compact acoustic network to create the traveling-wave phasing necessary for the operation in a Stirling cycle. The network has a coaxial geometry instead of the toroidal one usually used in such systems. The design, construction and performance measurements of the cooler are presented. A measured coefficient of performance relative to Carnot of 25% and a low temperature of −54 °C are achieved by the cooler. This efficiency surpasses the performance of the most efficient standing-wave cooler by almost a factor of two.

Keywords: Thermoacoustic (C); Stirling cooler (E)

1. Introduction

Since the beginning of 1980s until about 1999, most efforts in thermoacoustics have been focused on the development and understanding of standing-wave thermoacoustic systems [1–3]. These systems are relatively simple to design and build but because of the imperfect thermal contact between the working medium and the stack they are intrinsically irreversible. This means that these systems can not achieve high thermodynamic performance.

In 1979, Ceperley showed that the time phasing between pressure and gas velocity in the regenerator of a Stirling system is that of a traveling acoustic wave [4]. However, the first attempt of Ceperley to build a traveling thermoacoustic engine did not succeed. This was due mainly to the viscous losses in the regenerator as a consequence of the low acoustic impedance (high velocity). It is only in 1998 that the first working traveling-wave engine was demonstrated but at low efficiency [5].

The breakthrough in the development of thermoacoustic engines was realized by Backhaus et al. [6] in 1999 when they developed a traveling-wave thermoacoustic engine that achieved a measured thermal efficiency of 30%, corresponding to 41% of Carnot efficiency. They used a torus-shaped compact acoustic network to create the traveling-wave phasing necessary for the operation in a Stirling cycle. The high efficiency is achieved only after that the Gedeon and Rayleigh streaming were reduced to a minimum level [7].

Although much effort is done in developing traveling-wave thermoacoustic engines, there is little done for the development of traveling-wave thermoacoustic heat pumps. Poese et al. developed a traveling-wave thermoacoustic refrigerator for ice cream sales [8]. They used the same acoustic network as Backhaus et al. [7] in their refrigerator to create the appropriate phasing and high acoustic impedance. The only difference is that they used a hybrid acoustic-mechanical system instead of the acoustic network and resonator. This leads to a compact refrigerator that achieved a performance of 19% relative to Carnot.

The aim of this paper is to present a study of a coaxial traveling-wave (Stirling) cooler. The design, development, and performance measurements of the cooler will be presented. The remaining of this paper is organized as follows: Section 2 is devoted to the characteristics and design of the cooler. In Section 3, a description of the cooler is given.

* Corresponding author.
E-mail address: tijani@ecn.nl (M.E.H. Tijani).

0011-2275/$ - see front matter © 2008 Elsevier Ltd. All rights reserved.
doi:10.1016/j.cryogenics.2008.01.001

Section 4 describes the measurement procedure. Section 5 is devoted to the performance measurements. In the last section some conclusions related to the performance of the cooler are summarized.

2. Characteristics and design of the cooler

The cooler uses an acoustic network based on the same principle as that used by Backhaus et al. [7]. The only difference is that the present cooler uses a coaxial topology for the network instead of the toroidal one used by Backhaus et al. The coaxial configuration is compact and easy to construct.

The cooler uses the acoustic power produced by a linear motor to pump heat against a temperature gradient. Argon gas at an average pressure of 15 bar is used as the working medium at the operation frequency of 60 Hz. The thermoacoustic-Stirling cooler consists mainly of four parts: a linear motor, a 1/2-wavelength resonator, a regenerator unit, and an acoustic network.

The linear motor produces the acoustic power necessary for the heat pumping process. The resonator functions as a pressure vessel for the working gas, determines the acoustic resonance frequency and houses the regenerator unit. The regenerator unit consists of a regenerator, two heat exchangers, and a thermal buffer tube. The acoustic network, comprising a feedback inertance, a compliance, and an acoustic resistance creates the traveling-wave phasing necessary to operate in a Stirling cycle and feeds back the remnant acoustic power at the cold side to the ambient side. The regenerator and heat exchangers form an acoustic flow resistance. The regenerator unit is placed inside of the resonator at a location of high acoustic impedance (pressure antinode). The space created around the regenerator unit forms the acoustic network. The choice of an acoustic operating frequency of 60 Hz is dictated in part by the mechanical resonance frequency of the linear motor. This reason is one of the conditions necessary for optimal electroacoustic conversion efficiency of the linear motor. Argon gas is chosen because of the low sound velocity so that the length of the 1/2-wavelength is reasonably short. The resonator is designed in order to achieve an acoustic resonance of 60 Hz. The average pressure is chosen as high as possible for a high energy density in the system. On the other hand, choice of a high pressure will result in a small hydraulic radius for the regenerator. The regenerator is designed so that the hydraulic radius is small compared to the thermal penetration depth, the losses as low as possible, and to achieve a given cooling power at a given temperature. The optimal design of the cooler is realized with the computer code DeltaE [9]. In the next section the cooler will be described.

3. Description of the cooler

A schematic illustration of the thermoacoustic-Stirling cooler is shown in Fig. 1. A description of the different parts of the cooler will be given in the following.

3.1. Linear motor

A linear motor is chosen to drive the cooler because of the high electroacoustic conversion efficiency (80%) in comparison with moving coil loudspeakers (3–5%). Furthermore, a linear motor can produce much more acoustic power than a conventional loudspeaker. Originally, the linear motor was designed for another thermoacoustic system by *Q*drive [10]. However, because of the long time which may be involved with the development of a new motor, we decided to use this existing one. We anticipated that some matching problems between the driver and the cooler may arise. This may result in a lower performance of the motor. The linear motor consists of a permanent magnet which moves in the magnetic field generated by an electromagnet structure. A piston with a diameter of 7.62 cm is attached to the moving magnet so that the oscillating movement of the magnet can be transmitted to the gas in the resonator. The linear motor is placed in a housing to confine the pressurized gas. The design frequency of the motor is 60 Hz and it is determined by the moving mass of the motor, the mechanical stiffness, and the stiffness of the back volume of gas. A function generator in combination with a power amplifier feeds the linear motor.

3.2. Resonator

The resonator is designed in order to achieve an acoustic resonance frequency of 60 Hz. The resonator is made of stainless-steel and it has a total length of 2.89 m. The resonator consists of three sections as shown in Fig. 1. Starting at the driver side (left side), the first section is a pipe with a length of 30 cm and an inside diameter of 8.28 cm. The second section is a cone that adapts the 8.28 cm inside diameter pipe to a 9.55 cm inside diameter pipe and it has a length of 10 cm. The final section of the resonator which forms the main section is a pipe with a length of 2.49 m and an inside diameter of 9.55 cm. The small diameter pipe is used to adapt the linear motor with the large diameter pipe. The diameter of the large section of the resonator is determined by the diameter of the regenerator unit and the acoustic network that have to be housed inside the resonator.

3.3. Acoustic network

The compact acoustic network used to create the local traveling-wave phasing and the high acoustic impedance in the regenerator consists of the resistance of the regenerator unit, a compliance and a feedback inertance. A thin-wall cylindrical tube which forms a holder for the regenerator, heat exchangers, and the thermal buffer tube is placed at the right end of the large diameter pipe (cf. Fig. 1). The cylindrical volume of gas confined between the closed end of the resonator and the right side of the holder forms the acoustic compliance. The annular space between the resonator and the holder forms the feedback

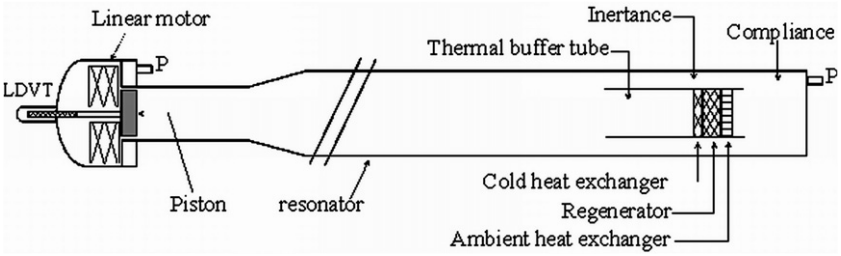

Fig. 1. Schematic illustration of the thermoacoustic-Stirling cooler.

inertance. The regenerator holder is attached to the cover plate used to close the end of the resonator. In this way the regenerator unit can be removed by removing the cover plate which is practical when exchanging parts during experiments. The cover plate contains also some feed-through for thermocouples, wires for the electrical heater used to generate heat load for the cooler, and tubing for the cooling water for the ambient heat exchanger.

3.4. Regenerator and heat exchangers

The regenerator consists of an 11 mm thick stack of 280 mesh twilled-weave stainless-steel screen punched at a diameter of 5.5 cm. The diameter of the screen wire is 28 μm. The stack is placed in a thin-wall tube (holder). The calculated hydraulic radius of the regenerator is about 22 μm which is smaller than the argon's thermal penetration depth (about 90 μm at 300 K).

The water cooled ambient heat exchanger is of the type tube-and-shell design with a diameter of 55 mm. The tubes, which are parallel to the acoustic displacement, carry argon gas. The tubes have a diameter of 2 mm and a length of 15 mm. They are cooled by chilled water passing through channels perpendicular to the tubes.

A spiral electrical heater is placed at the cold side of the regenerator to simulate cooling power. The spiral heater has a diameter of 55 mm. The diameter of the heater wire is 1.6 mm and it has a heating power of 240 W.

4. Measurement procedure and performance

The characterization of the performance of the cooler requires knowledge of many quantities like temperatures, dynamic pressures at different locations of the system, and displacement of the piston. In the following a description of the instrumentation used for the measurements and the expressions used to determine the different powers are given.

4.1. Instrumentation

Several type-K thermocouples with a diameter of 0.5 mm are used to measure the temperature at different locations in the cooler. Three thermocouples are used to measure the temperature through the regenerator and are centered radially: one at the cold side, one at the centre, and one at the ambient side. The axial temperature profile within the regenerator is used to detect Gedeon streaming [7]. Two other thermocouples are placed equidistant on the inside wall of the thermal buffer tube. The temperature profile measured by these two thermocouples is used to detect the presence of either Rayleigh or jet-driven streaming [7]. Finally, two 2 mm-thick thermocouples are used to measure the inlet and outlet temperatures of the water stream supplying the ambient heat exchanger. Several piezoresistive pressure sensors are placed throughout the system. One pressure sensor is placed at the location of the piston of the linear motor to measure the dynamic pressure at that location. One pressure sensor is placed on the end plate of the resonator to measure both static and dynamic pressure. Two other pressure sensors are placed on the resonator just at the front of the heat pump unit to measure the effective acoustic power input to the heat pump part using the two-microphone method [11]. The acoustic power input produced by the linear motor can be deduced from the measurement of the dynamic pressure and the volumetric velocity at the piston location. The velocity of the piston is deduced from the displacement measurement of the piston. A displacement sensor (LVDT), mounted on the back of the piston, is used to measure the displacement.

4.2. Powers

The determination of the performance of the cooler requires the knowledge of different powers and temperatures in the system. The acoustic pressure and displacement measurements are made with a lock-in amplifier. The thermocouples signals are read by a data logger and sent to a computer for record and display. In the following the different powers will be defined.

The acoustic power input from the linear motor is given by

$$\dot{W} = \frac{1}{2} puA \cos\varphi, \tag{1}$$

where p is the amplitude of the dynamic pressure at the location of the piston, u is the velocity of the piston, A is the area of the piston, and φ is the phase difference between p and u. The velocity is deduced from the displacement through $u = \omega d$, where d is the peak displacement of the piston and ω is the angular frequency.

The heat load is simulated by an electrical heater which is used as a cold heat exchanger. A power supply is used to apply electric power to the heater and generates heat load given by

$$\dot{Q}_c = VI, \tag{2}$$

where V is the voltage across the heater and I is the current. The heat extracted at the ambient side of the regenerator by cooling water flowing through the ambient heat exchanger is given by

$$\dot{Q}_a = \rho c_p U (T_{out} - T_{in}), \tag{3}$$

where ρ is the density of water, c_p is the specific heat, U is the volume flow rate of water, and T_{in} and T_{out} are the input and output temperatures of the water stream flowing through the ambient heat exchanger. The volume flow rate is measured with a turbine flow meter.

4.3. Performance indicators

The performance of the cooler, also called the coefficient of performance (COP), is given by

$$\mathrm{COP} = \frac{\dot{Q}_c}{\dot{W}}, \tag{4}$$

where W and Q_c are given in (1) and (2). The Carnot coefficient of performance is the maximal theoretical performance a cooler can achieve and it is given by

$$\mathrm{COPC} = \frac{T_c}{T_a - T_c}, \tag{5}$$

where T_c is the temperature of the cold heat exchanger and T_a is the temperature of the ambient heat exchanger. The coefficient of performance relative to Carnot is defined as the ratio

$$\mathrm{COPR} = \frac{\mathrm{COP}}{\mathrm{COPC}}. \tag{6}$$

The experimental results will be presented in the following section for different drive ratio's. The drive ratio is defined as the ratio of the dynamic pressure amplitude at the piston location and the mean pressure of the gas.

4.4. Performance measurements

A cool-down measurement at a drive ratio of 4% is shown in Fig. 2. Initially, the cooler was at room temperature and once the linear motor is switched on, the temperature of the cold side drops quickly and reaches a low temperature of −54 °C without any thermal insulation on the cold side. The cooler needs only 2 min to reach such a low temperature. Because of the coaxial topology used for the cooler it is not possible to use thermal insulation at the cold side in the present design. Using insulation will block the inertance flow area which will result in a malfunction of the cooler.

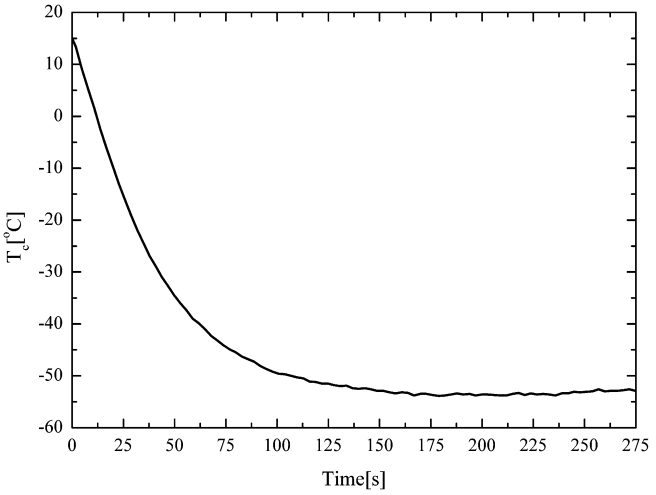

Fig. 2. Temperature of the cold heat exchanger as function of time.

Fig. 3 shows the cold end temperature as function of the heat load for three different drive ratio's. T_c is a linearly increasing function of the heat load. High drive ratio's lead to low temperatures and high heat loads.

Fig. 4 shows the COP and COPR as function of the heat load for three different drive ratio's. For all drive ratio's, the COP increases as the heat load increases. The slope of the COP curves decreases as the drive ratio increases. The COPR shows a parabolic behavior with a maximum which shifts to higher heat loads as the drive ratio increases. The maximum COPR achieved with the cooler is 25% at $Q_c = 25$ W and $T_c = -11$ °C for a drive ratio of 4.3%. As the cooler is not thermally insulated there may be a heat leak from the environment and from the ambient side of the regenerator to the cold side. However, the heat leak has not been determined experimentally but it can be estimated to about 5 W at the operating point.

An elastic membrane has been placed at the ambient heat exchanger to suppress Gedeon streaming. It is difficult

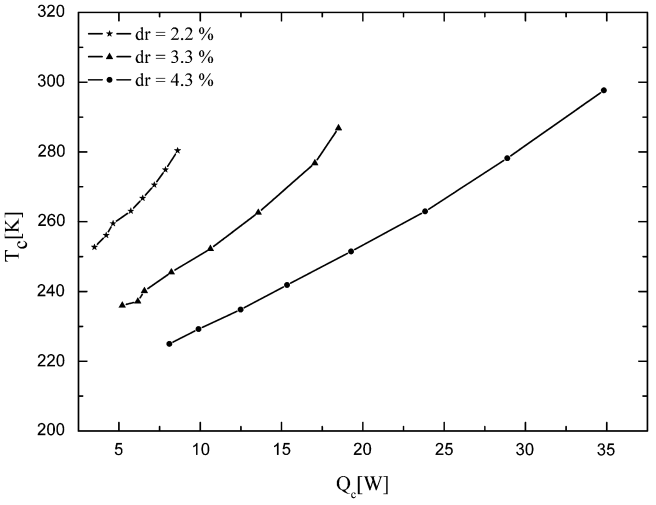

Fig. 3. Temperature of the cold heat exchanger as function of the heat load.

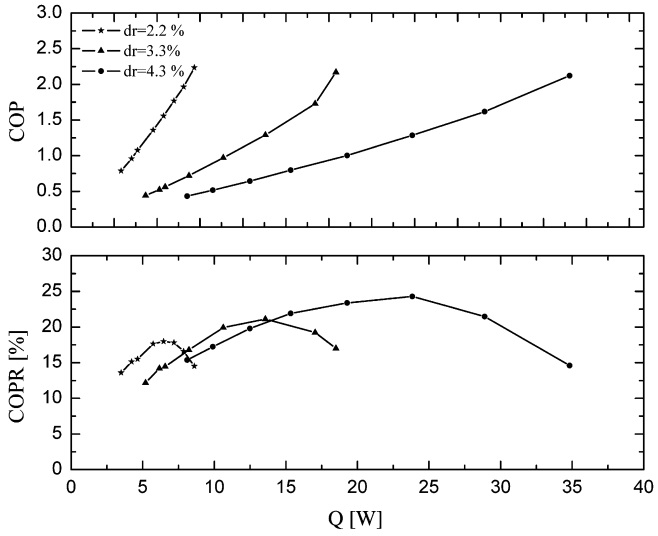

Fig. 4. Measured COP and COPR as function of the heat load for three different drive ratio's.

to detect the presence of Rayleigh or jet-driven streaming by monitoring the temperature profile in the thermal buffer tube. However, a lower cold temperature is realized when a flow straightener made of nickel foam is placed at the end of the thermal buffer tube.

The acoustic power dissipated in the resonator is measured as function of the drive ratio after the regenerator unit has been removed from the resonator. In this case the acoustic power input from the linear motor must compensate for the power dissipated in the resonator by thermo-viscous processes at the wall. In Fig. 5, the acoustic power dissipated in the resonator is plotted against the drive ratio squared. The acoustic power dissipated in the resonator increases as the drive ratio increases as expected. The uncertainty of these measurements is about ±5%. At

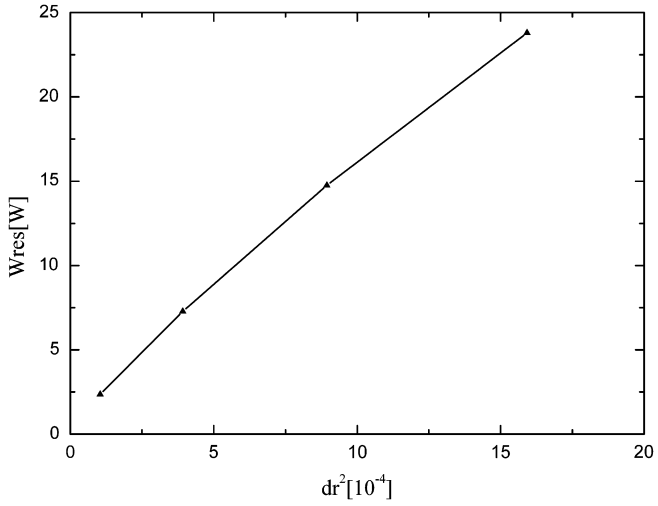

Fig. 5. Measured acoustic power dissipated in the resonator (without regenerator unit) as function of the drive ratio squared.

the operating point of high performance (dr = 4.3%) the losses in the resonator part between the linear motor and the heat pump amount about 10 W. This is about half the power input. Considering only the power input to the heat pump part (excluding the resonator losses) a COPR of 45% is deduced. This means that the cooler is operating properly in a Stirling cycle. To improve the performance of the cooler as whole the losses in the resonator have to be minimized by using for example a quarter-wavelength resonator. There is also a matching problem between the driver and the cooler which limits the acoustic power input to maximal 25 W at dr = 4%. There are some possibilities to improve the matching between the linear motor and the cooler for example by changing the piston area and/or the operating frequency or by using a new linear motor which match the cooler. This issue is under study along with the possibility of using a quarter-wavelength resonator where the driver is placed at a high impedance position. Also the possibility of using a mechanical resonator (a mass-spring system) instead of the acoustic resonator will be explored. A further improvement of the performance of the cooler can be achieved by using thermal insulation at the cold side of the cooler, and by improving the heat exchangers. A fin-tube heat exchanger is also under study and will be used instead of the shell-tube one. These improvements will be the subject of a future work. After incorporating these improvements we expect a COPR of about 35%. The cooler may be used for cryogenic applications down to about 150 K provided that the power input from the driver is high enough [12].

5. Conclusions

A coaxial thermoacoustic-Stirling cooler is built and performance measurements are performed. The cooler achieved a coefficient of performance relative to Carnot of 25% at $Q_c = 25$ W and $T_c = -11$ °C and a low temperature of −54 °C without heat load. This efficiency surpasses the performance of the most efficient standing-wave cooler by almost a factor of two. About a half of the acoustic power input to the cooler is dissipated in the resonator. Reduction of the resonator losses by using a quarter-wavelength resonator will result in a COPR of about 35%. Further improvements of the performance of the cooler may be achieved by optimizing the matching between the driver and cooler, by using thermal insulation at the cold side of the cooler, and by improving the heat exchangers.

Acknowledgements

This work has been funded by SenterNovem (Dutch agency for sustainable development and innovation) within the EOS-LT program.

References

[1] Hofler TJ. Thermoacoustic refrigerator design and performance. Ph.D. dissertation, Physics Department, University of California at San diego; 1986.

[2] Garrett S, Adeff JA, Hofler TJ. Thermoacoustic refrigerator for space applications. J Thermophys Heat transfer 1993;7:595.

[3] Tijani MEH, Zeegers JCH, de Waele ATAM. Construction and performance of a thermoacoustic refrigerator. Cryogenics 2002;42: 59–66.

[4] Ceperley PH. A pistonless Stirling engine – the traveling wave heat engine. J Acoust Soc Am 1979;66:1508–13.

[5] Yazaki T, Iwata A, Maekawa T. Traveling wave thermoacoustic heat engine in looped tube. Phys Rev Lett 1998;81:3128–31.

[6] Backhaus S, Swift GW. A thermoacoustic Stirling heat engine. Nature (London) 399 1999;107:335–8.

[7] Backhaus S, Swift GW. A thermoacoustic Stirling heat engine: detailed study. J Acoust Soc Am 2000;107:3148–66.

[8] Poese ME, Smith R, Garrett S. Regenerator-base thermoacoustic refrigerator for ice cream storage applications. J Acoust Soc Am 2003;114:2328.

[9] Ward W, Swift GW. Design environment for low amplitude thermoacoustic engine. J Acoust Soc Am 1994;95:3671.

[10] CFIC Inc./Qdrive, 302 Tenth Street, Troy, NY 12180, USA.

[11] Fusco AM, Ward WC, Swift GW. Two-sensor power measurement in lossy ducts. J Acoust Soc Am 1992;91:2229–35.

[12] Swift GW, Gardner DL, Backhaus S. Acoustic recovery of lost power in pulse tube refrigerators. J Acoust Soc Am 1998;105:711–24.